Cell Reports

Article

Metabolic reprogramming of *Pseudomonas aeruginosa* by phage-based quorum sensing modulation

Graphical abstract

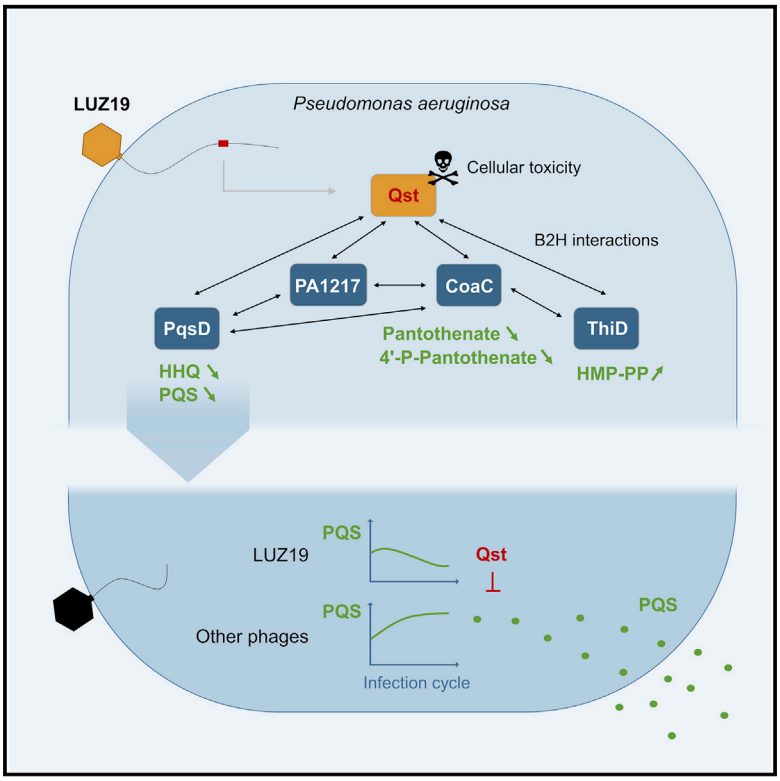

Highlights

- *Pseudomonas* phage LUZ19 encodes a quorum sensing targeting protein, Qst
- Qst targets the PQS system by binding the key biosynthesis enzyme PqsD
- The interaction causes reduced PQS level and provides an efficient LUZ19 infection
- Study of Qst reveals a functional interaction network in *Pseudomonas aeruginosa*

Authors

Hanne Hendrix,
Maria Zimmermann-Kogadeeva,
Michael Zimmermann, ...,
Jean-Paul Noben, Abram Aertsen,
Rob Lavigne

Correspondence

rob.lavigne@kuleuven.be

In brief

Hendrix et al. report a phage protein that targets the PQS quorum sensing system for host-hijacking by directly binding a PQS biosynthesis enzyme. Moreover, by studying this protein, they reveal an interaction network in *Pseudomonas aeruginosa* that links quorum sensing to a non-ribosomal peptide synthetase pathway and cofactor biosynthesis pathways.

Hendrix et al., 2022, Cell Reports *38*, 110372
February 15, 2022
https://doi.org/10.1016/j.celrep.2022.110372

CellPress

Cell Reports

CellPress
OPEN ACCESS

Article

Metabolic reprogramming of *Pseudomonas aeruginosa* by phage-based quorum sensing modulation

Hanne Hendrix,[1] Maria Zimmermann-Kogadeeva,[2,6] Michael Zimmermann,[2,7] Uwe Sauer,[2] Jeroen De Smet,[1,8] Laurens Muchez,[3] Maries Lissens,[1] Ines Staes,[4] Marleen Voet,[1] Jeroen Wagemans,[1] Pieter-Jan Ceyssens,[1,9] Jean-Paul Noben,[5] Abram Aertsen,[4] and Rob Lavigne[1,10,*]

[1]Laboratory of Gene Technology, Department of Biosystems, KU Leuven, 3001 Heverlee, Belgium
[2]Institute of Molecular Systems Biology, ETH Zurich, 8092 Zürich, Switzerland
[3]Centre for Surface Chemistry and Catalysis, Department of Microbial and Molecular Systems, KU Leuven, 3001 Heverlee, Belgium
[4]Laboratory of Food Microbiology, Department of Microbial and Molecular Systems, KU Leuven, 3001 Heverlee, Belgium
[5]Biomedical Research Institute and Transnational University Limburg, School of Life Sciences, Hasselt University, 3590 Diepenbeek, Belgium
[6]Present address: European Molecular Biology Laboratory, Genome Biology Unit, 69117 Heidelberg, Germany
[7]Present address: European Molecular Biology Laboratory, Structural and Computational Biology Unit, 69117 Heidelberg, Germany
[8]Present address: Lab4Food, Department of Microbial and Molecular Systems, KU Leuven, 2240 Geel, Belgium
[9]Present address: Unit of Human Bacterial Diseases, Sciensano, 1050 Brussels, Belgium
[10]Lead contact
*Correspondence: rob.lavigne@kuleuven.be
https://doi.org/10.1016/j.celrep.2022.110372

SUMMARY

The *Pseudomonas* quinolone signal (PQS) is a multifunctional quorum sensing molecule of key importance to *P. aeruginosa*. Here, we report that the lytic *Pseudomonas* bacterial virus LUZ19 targets this population density-dependent signaling system by expressing quorum sensing targeting protein (Qst) early during infection. We demonstrate that Qst interacts with PqsD, a key host quinolone signal biosynthesis pathway enzyme, resulting in decreased levels of PQS and its precursor 2-heptyl-4(1H)-quinolone. The lack of a functional PqsD enzyme impairs LUZ19 infection but is restored by external supplementation of 2-heptyl-4(1H)-quinolone, suggesting that LUZ19 exploits the PQS system for successful infection. We establish a broad functional interaction network of Qst, which includes enzymes of cofactor biosynthesis pathways (CoaC/ThiD) and a non-ribosomal peptide synthetase pathway (PA1217). Qst therefore represents an exquisite example of intricate reprogramming of the bacterium by a phage, which may be further exploited as tool to combat antibiotic resistant bacterial pathogens.

INTRODUCTION

Bacteriophages are the most abundant biological entities on Earth, affecting bacteria and even global ecosystems through microbial mortality (Suttle, 2007), horizontal gene transfer (McDaniel et al., 2010), and metabolic reprogramming (De Smet et al., 2016). Due to the intimate co-evolution with bacteria, phages can efficiently and extensively affect physiological processes in the host. This hijacking primarily takes place immediately after infection, and is observed across the entire metabolic network (De Smet et al., 2017). At the molecular level, this hijacking can be achieved through protein-protein interactions of phage proteins that inhibit, activate, or functionally alter specific host proteins at the early stage of infection (Häuser et al., 2012; Roucourt and Lavigne, 2009). These early-expressed phage proteins also can include metabolic enzymes, which can complement rate-limiting host enzymes to compensate for metabolic imbalances arising during infection, or more generally interact with the host's central metabolic pathways to achieve metabolic reprogramming (Hurwitz et al., 2013; Thompson et al., 2011).

The host takeover is not self-evident, and is preceded by a struggle for cellular control between the phage and the host (Samson et al., 2013). A recently identified defense strategy against phage predation is the use of quorum sensing systems by *Pseudomonas aeruginosa* (Hoyland-Kroghsbo et al., 2013, 2017). Since quorum sensing is population density-dependent, this is consistent with the fact that the risk of phage infection is the highest at high cell density. Known phage resistance mechanisms regulated by quorum sensing are the reduction of phage receptors on the cell surface (Hoyland-Kroghsbo et al., 2013) and the activation of the prokaryotic adaptive CRISPR-Cas immune system (encoded by the Clustered Regularly Interspaced Short Palindromic Repeats loci and CRISPR-associated (Cas) genes) (Patterson et al., 2016; Hoyland-Kroghsbo et al., 2017). Generally, quorum sensing influences the physiological state of cells to better protect them against phage attack (Qin et al., 2017).

In *P. aeruginosa*, three main quorum sensing systems have been identified to date: the two N-acylhomoserine lactones (AHL)-dependent systems *lasI*/*lasR* and *rhlI*/*rhlR* (Pesci et al., 1997), and the *Pseudomonas* quinolone signal (PQS) system *pqsABCD, pqsH*/*pqsR* (Dubern and Diggle, 2008). These

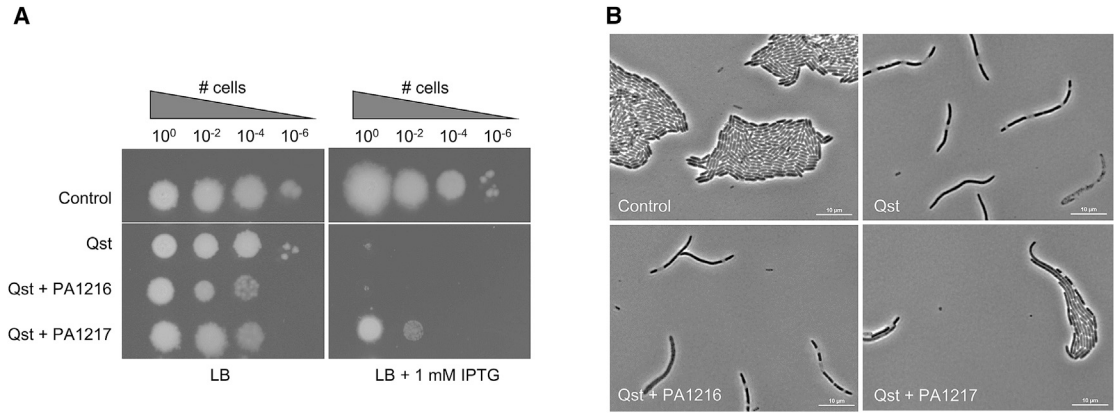

Figure 1. Antibacterial effect of the early phage protein Qst on *P. aeruginosa* PAO1 growth and its partial complementation by the hypothetical protein PA1217

(A) Hundredfold serial dilutions of *P. aeruginosa* PAO1 strains harboring the *qst* gene (second row), both *qst* and *PA1216* genes (third row), and both *qst* and *PA1217* genes (bottom row) were spotted on medium with (right) or without (left) IPTG induction, together with a negative control (empty vector construct, top row).

(B) *P. aeruginosa* PAO1 morphology after Qst expression (top right), and both Qst and PA1216/PA1217 expression (bottom), together with a control (empty vector construct, top left). Microscopic recording of *P. aeruginosa* cells after growth for 5 h in the presence of 1 mM IPTG. The scale bars represent 10 μm.

signaling systems can regulate the expression of up to 10% of *Pseudomonas* genes, including self-regulation (autoinduction), cross-regulation between the different quorum sensing systems, and regulation of bacterial virulence and biofilm formation (Schuster et al., 2003; Williams and Camara, 2009). Remarkably, the function of almost half of the quorum sensing-regulated genes remains unknown (Schuster et al., 2003). Besides cell density, the quorum sensing systems also can be influenced by environmental factors, such as oxidative stress (Haussler and Becker, 2008). For example, the PQS system plays a key role in protecting a micro-colony by both stimulating the destruction of damaged sister cells and rescuing undamaged members from oxidative stress by lowering their metabolic activity (D'Argenio et al., 2002; Haussler and Becker, 2008). Although recent studies suggest an important role of the PQS signal in the *P. aeruginosa* response to phage infection (Blasdel et al., 2018; Bru et al., 2019; De Smet et al., 2016), no mechanisms to interfere with PQS signaling have been discovered in phages so far.

In this study, we aimed at investigating the mechanism of phage interaction with PQS signaling using the podovirus LUZ19 of the *Autographiviridae* family, for which the genome organization has been intensely studied (Adriaenssens et al., 2020; Lavigne et al., 2013). We identified a protein expressed during early infection, gp4 (termed Qst, "quorum sensing targeting protein"), which modulates the PQS levels together with certain host metabolites, inhibiting cell division in *P. aeruginosa* cells. We demonstrate that this metabolic reprogramming is associated with acetyl-coenzyme A (CoA) metabolism and is achieved by a complex interaction network, in which Qst interacts with enzymes of both cofactor biosynthesis pathways and two secondary metabolite pathways: (1) the well-known quorum sensing molecule PQS, and (2) a predicted non-ribosomal peptide (from the PA1221 cluster; Gulick, 2017). The protein of the non-ribosomal peptide synthetase (NRPS) cluster is tightly regulated by quorum sensing and can neutralize the antibacterial effect of Qst, suggesting a phage-mediated effect on cell signaling. Further exploration of these phage-host interactions may aid in the development of new antibacterial therapies targeting quorum sensing.

RESULTS

An early-expressed phage LUZ19 protein shows antibacterial activity in *P. aeruginosa*, which is complemented by the quorum sensing-regulated acetyltransferase PA1217

In a systematic screen for small growth-inhibitory genes in *P. aeruginosa* PAO1-infecting phages, we identified the early-expressed protein gp4 of phage LUZ19 (referred to hereafter as Qst). Qst has a predicted molecular weight of 13 kDa, has no conserved domains, and is only found in *Phikmvvirus* phages. We observed that induction of *qst* expression completely abolished *P. aeruginosa* growth (Figures 1A and S1A), resulting in a filamentous growth type (Figure 1B). Interestingly, this toxicity is rather specific, as *E. coli* MG1655 cells grew normally after episomal expression of Qst (Figure S1B).

To study the mechanisms underlying this toxicity, we performed a complementation screen to identify bacterial proteins that can alleviate this toxic effect upon overexpression. The 20 confirmed positive clones containing random *P. aeruginosa* PAO1 genome fragments all matched to a single locus in the *Pseudomonas* genome, with five different fragments that overlapped by 3,227 base pairs (bp) (position 1,316,424–1,319,651 bp, minus-strand) encoding two putative ORFs, PA1216 and PA1217. Co-expression of either PA1216 or PA1217 with Qst in *P. aeruginosa* PAO1 revealed that only PA1217, but not PA1216, can partially mitigate the toxic effect of the phage protein on the host cells (Figures 1A and 1B). PA1217 is a predicted 2-isopropylmalate synthase embedded in an uncharacterized NRPS cluster. Although no products of this biosynthetic cluster have currently been described, the cluster is known to be tightly regulated by quorum sensing (Chugani

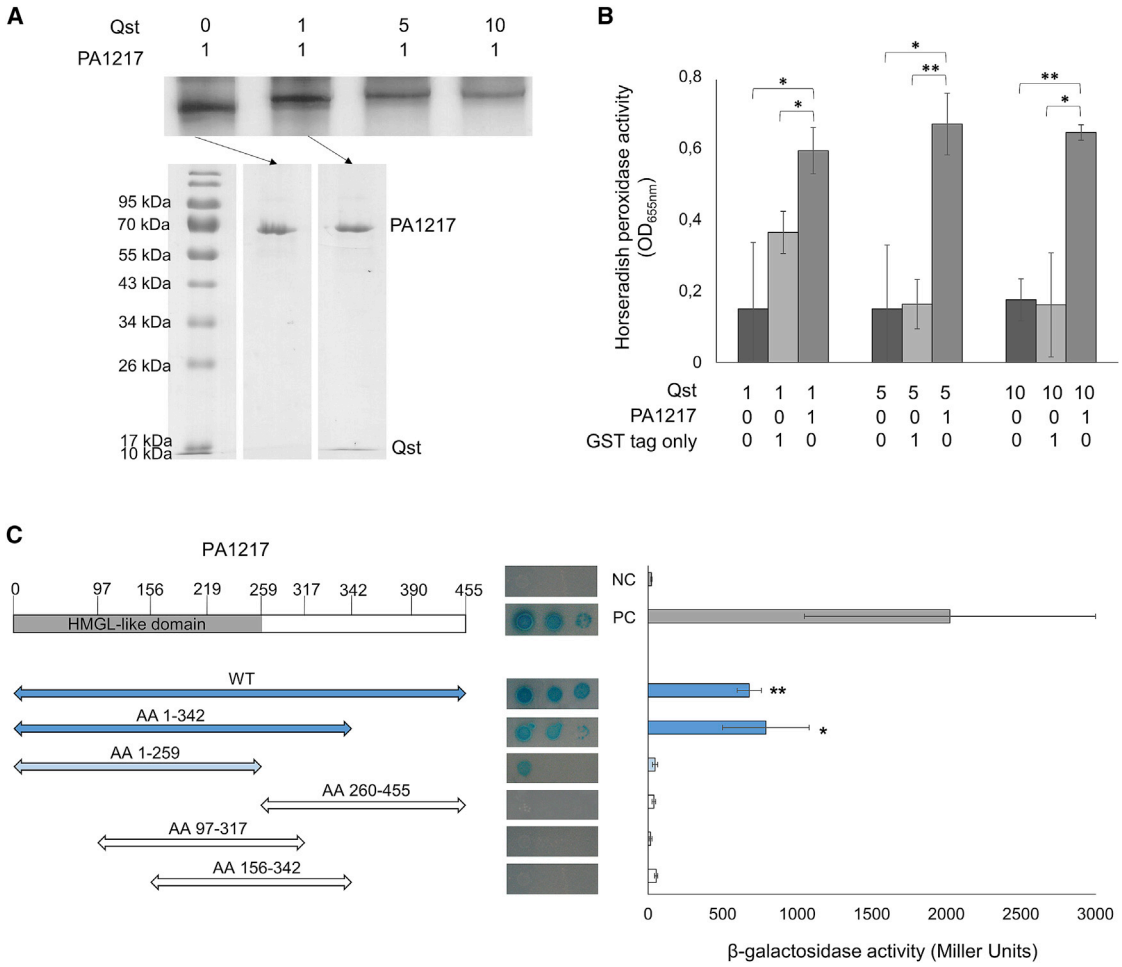

Figure 2. Interaction analyses of Qst and the *P. aeruginosa* hypothetical protein PA1217

(A) Native gel mobility shift assay using an equal amount of PA1217 and an increasing amount of Qst (top). The numbers indicate the relative amount of Qst and PA1217 (1 corresponds to 4 pmol). The band in the first lane and the shifted band in the second lane were excised and analyzed via SDS-PAGE (bottom). The two bands on the SDS-PAGE were confirmed by mass spectrometry analysis to be PA1217 and Qst.

(B) ELISA using an equal amount of GST-tagged PA1217 (1 corresponds to 10 pmol) as bait and an increasing amount of His-tagged Qst as prey. As negative controls, no bait protein and an unfused GST tag were used. The numbers indicate the relative amount of Qst, PA1217, and GST tag. The Y axis indicates the absorbance measured at OD_{655nm} after 10 min, using anti-mouse IgG antibody conjugated to horseradish peroxidase and 1-Step Slow TMB-ELISA substrate. Error bars represent SD, and p values (compared with no bait protein and GST tag separately) were calculated using the Student's t test (n = 3), *p < 0.05, **p < 0.01.

(C) Bacterial two-hybrid assay in which the T18 domain is N-terminally fused to Qst and the T25 domain is N-terminally fused to PA1217 or a fragment of PA1217. Fragments of the PA1217 protein are shown on the left. Blue and white arrows indicate fragments with a positive and no signal, respectively. Interactions were visualized by a drop test on minimal medium (pictures in the middle), and quantified by measuring the β-galactosidase activity, which are indicated in Miller Units (graph at the right; see also Figure S2). Non-fused T25 and T18 domains were used as a negative control, and the leucine zipper of GCN4 was used as a positive control. Error bars represent SD, and p values (compared with both combinations with empty counterparts, Figure S2) were calculated using the Student's t test (n = 3), *p < 0.05, **p < 0.01.

et al., 2012; Rampioni et al., 2016; Schuster et al., 2003; Wagner et al., 2003).

Subsequent protein-protein interaction studies confirmed that Qst directly interacts with PA1217. A native gel mobility shift assay with an equal amount of recombinant PA1217 and an increasing amount of Qst protein displayed a small but distinct shift in PA1217 migration in presence of Qst (Figure 2A). Furthermore, an ELISA using PA1217 as bait and Qst as prey validated the interaction (Figure 2B). *In vivo*, a bacterial two-hybrid assay revealed significant ($p < 0.05$) positive reactions for Qst with both the full PA1217 protein and its N-terminal domain (residues 1–342), containing a catalytic HMGL (hydroxymethylglutaryl-coenzyme A lyase)-like domain (residues 1–259; Pfam, E-value: 1.2×10^{-61}). Intriguingly, the HMGL-like domain alone did not bind Qst, which might be due to a lack of proper folding of the protein fragment (Figures 2C and S2).

The *P. aeruginosa* protein PA1217 is predicted to be a 2-isopropylmalate synthase. One functional homolog in *P. aeruginosa* is reported, LeuA, which catalyzes the first step in leucine biosynthesis. To verify the 2-isopropylmalate synthase

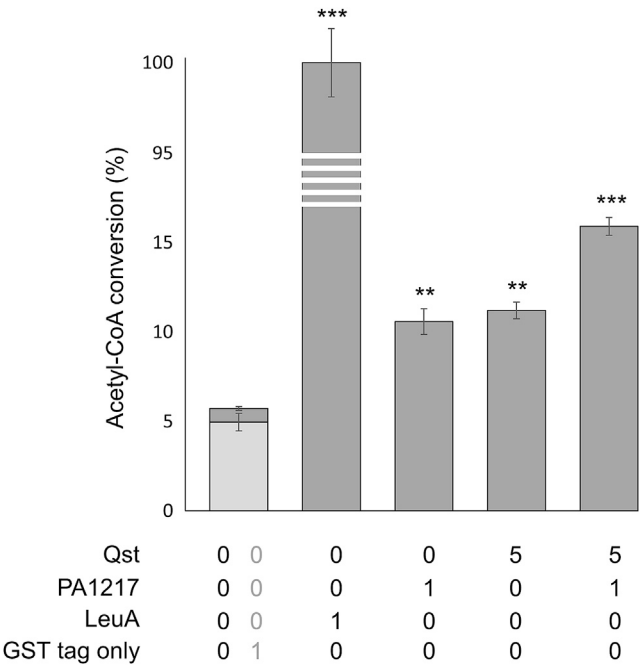

Figure 3. CoA acetyltransferase activity assay

The acetyl-CoA transferase activity was measured using the Ellman's reagent (DTNB) after 30 min incubation at 37°C, and expressed relative to the activity of the *P. aeruginosa* 2-isopropylmalate synthase LeuA. Error bars represent SD, and p values (compared with both controls) were calculated using the Student's t test (n = 3), **p < 0.01, ***p < 0.001. The numbers below indicate the relative amount of the proteins, i.e., 1 μg of PA1217 and 5 μg of Qst, that were used in the reaction mixtures. See also Figure S3.

activity of PA1217, we assayed acetyl-CoA to CoA conversion *in vitro* using 3-methyl-2-oxobutanoic as a substrate (Roucourt et al., 2009), and purified LeuA as a positive control. Although both LeuA and PA1217 showed transferase activity, the activity of PA1217 was markedly lower, suggesting a different natural substrate (Figure 3). We confirmed this observation by *^{1}H-NMR* analysis, which revealed that the reaction products were only formed by LeuA, while PA1217 merely consumed acetyl-CoA (Figure S3). This potential alternative substrate specificity of PA1217 may be explained by its predicted role in the production or modification of a non-ribosomal peptide. This hypothesis is further supported by the fact that homologs of 2-isopropylmalate synthases were identified in other NRPS clusters (Jenul et al., 2018; Rouhiainen et al., 2010). Following up on the Qst-PA1217 interaction analysis, we tested whether Qst has an inhibitory effect on the enzymatic activity of PA1217. Surprisingly, we found that purified Qst was also able to consume acetyl-CoA, and the combination of Qst and PA1217 showed additive enzymatic activity (Figures 3 and S3). These data suggest that the small, early-expressed phage protein Qst interferes with acetyl-CoA metabolism in the host cell.

Untargeted metabolomics reveals alterations in the central carbon metabolism and the PQS pathway

To further investigate the function of Qst, we used untargeted metabolomics to identify host metabolic pathways that are either directly or indirectly affected by this protein. We compared metabolite levels between *P. aeruginosa* PAO1 expressing recombinant Qst and the wild-type strain, the strain overexpressing PA1217, or the strain expressing both Qst and PA1217. In a time course experiment, we measured the levels of 1,140 known metabolites (from the Kyoto Encyclopedia of Genes and Genomes database [Kanehisa and Goto, 2000]) before and after Qst expression (at 15, 30, 45, 60, 90, and 120 min) (Table S1). Upon Qst expression, only nine metabolites changed significantly (abs(log2(FC)) $\geq$ 1 and p value < 0.05) in at least one time point of the experiment compared with the wild-type strain and showed a significant change over time (Page's trend test: false discovery rate [FDR] < 0.05), as shown in the heatmap of fold changes (Figure 4A, Table S1). Upon induced PA1217 expression, these changes were mostly abolished.

The list of significantly changed metabolites includes pantothenate and 4-phosphopantothenate, which are precursors for biosynthesis of cofactors coenzyme A (CoA) and 4-phosphopantetheine. Another metabolite that is significantly reduced upon Qst expression is lipoate, which functions as an acyl carrier cofactor similar to CoA and 4-phosphopantetheine (Hazra et al., 2009; Spalding and Prigge, 2010). Together, these findings indicate that Qst likely affects acyltransferase metabolism. The observed reduction in cofactor precursors could result from the overconsumption of acyl carrier factors (indirect effect), or from the overactivation of biosynthesis enzymes (through direct interaction). Of note, 4-phosphopantetheine is an essential cofactor for peptidyl carrier proteins, such as the NRPS PA1221, which belongs to the same secondary metabolite biosynthesis gene cluster as PA1217 (Mitchell et al., 2012). Furthermore, the CoA biosynthesis pathway is known to influence the thiamine biosynthesis pathway, which could explain the increase of 2-methyl-4-amino-5-hydroxymethylpyrimidine diphosphate, a precursor of thiamine pyrophosphate (Enos-Berlage and Downs, 1997).

Another important observation is the decreased abundance of the quorum sensing molecule 2-heptyl-4(1H)-quinolone (HHQ) upon Qst expression (Figures 4A and S4A). This molecule is synthesized by the gene products of *pqsABCDE* (Figure 4B), and is a precursor of the quorum sensing molecule 2-heptyl-3-hydroxy-4(1H)-quinolone (PQS), which is also decreased (log2(FC) ≤ -1 and p value < 0.07) in all time points after Qst expression (Table S1, Figure S4A). However, it should be noted that both changes occur prior to Qst induction, which might be the result of leaky control of the protein expression (Choi et al., 2005). This is also observed in the spot assay, which demonstrated that growth of the *P. aeruginosa* strain harboring the *qst* gene is altered without isopropyl-β-D-1-thiogalactopyranoside (IPTG) induction (Figure 1A). Furthermore, the temporal profile of PQS in the double expression mutant suggests an initial decrease by Qst, which is subsequently complemented by PA1217 (Figure S4A). These results were supported by the results from a bioassay using the *P. aeruginosa* PAO1-R1 (pTS400) *lacZ* reporter strain, hinting to a lower concentration of alkyl quinolones, such as PQS or HHQ, present in the supernatant from *P. aeruginosa* cells expressing Qst compared with the strain expressing both Qst and PA1217 (Figure S4B). To exclude growth effects and directly link Qst expression levels

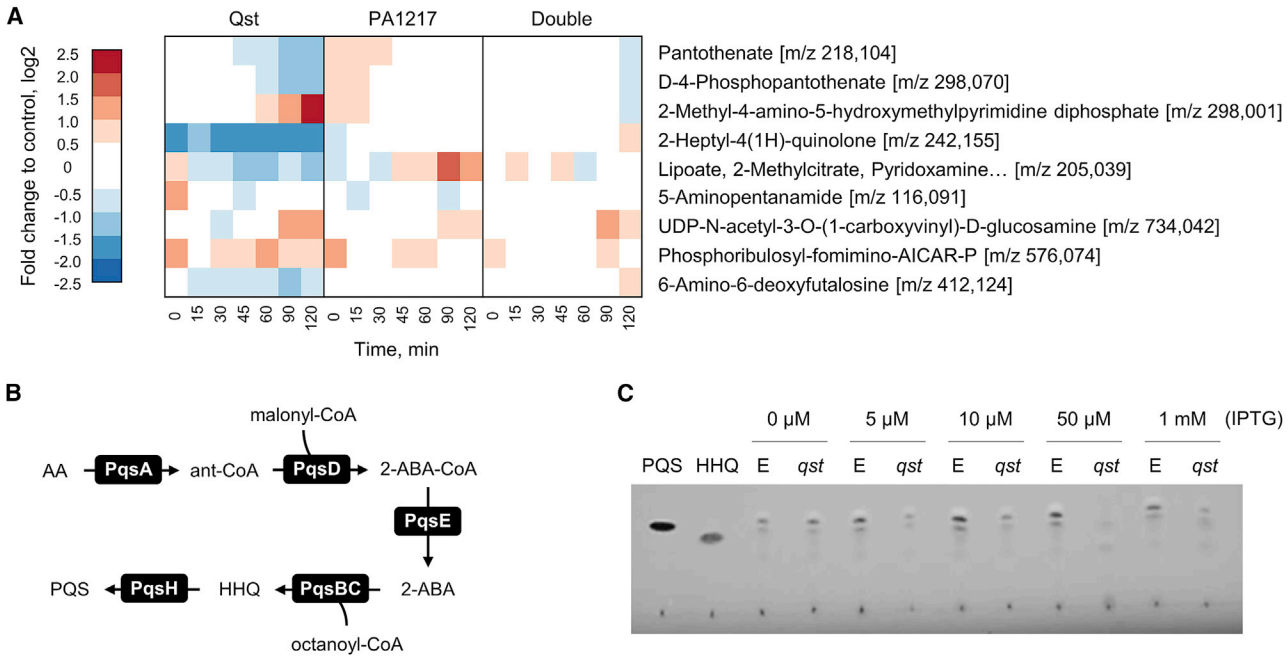

Figure 4. Impact of Qst on metabolite levels in *P. aeruginosa*

(A) Heatmap of significantly changed metabolites after recombinant Qst expression. Only metabolites that meet the following criteria are shown: Page FDR < 0.05, and at least one time point with an abs(log2(FC)) ≥ 1 and p value < 0.05 (both compared with the wild type). Levels of selected metabolites in a *P. aeruginosa* PAO1 strain overexpressing PA1217, and in a strain co-expressing Qst and PA1217 (double) are shown as well. Fold changes represent the means of three biological replicates. See also Figure S4A and Table S1.

(B) Schematic overview of the PQS biosynthetic pathway. AA, anthranilic acid; Ant-CoA, anthraniloyl-coenzyme; 2-ABA-CoA, 2-aminobenzoylacetyl-CoA; 2-ABA, 2-aminobenzoylacetate; HHQ, 2-heptyl-4(1H)-quinolone; PQS, 2-heptyl-3-hydroxy-4(1H)-quinolone.

(C) Thin-layer chromatography of cell extracts from *P. aeruginosa* cells expressing different levels of Qst. Alkyl quinolones were extracted from 24 h old cell cultures of *P. aeruginosa* PAO1 strains containing an empty pUC18mini construct E or a pUC18mini construct with *qst* gene (*qst*), induced with different IPTG concentrations. As controls, 10 mM synthetic PQS and HHQ were used. See also Figure S5.

to reduced levels of PQS, thin-layer chromatography was performed on the cell lysate from *P. aeruginosa* cells induced with different IPTG concentrations, including the sub-growth-inhibitory concentration (Figure S5A). The assay revealed reduced PQS levels upon increasing Qst expression levels (Figures 4C and S5B), confirming the observed impact of Qst on the quorum sensing molecule.

Qst interacts with both quorum sensing-associated secondary metabolite biosynthesis and central metabolism pathways

Based on the observed influence of Qst on a range of metabolic pathways revealed by metabolomics analysis, we hypothesized that Qst also interacts with other enzymes beyond PA1217. To identify such additional interaction partners, we performed an *in vitro* pull-down assay using immobilized His-tagged Qst protein as bait and crude *Pseudomonas* cell lysate as prey. The elution fractions showed additional protein bands compared with the control sample (Figure S6A). We analyzed both samples by electrospray ionization tandem mass spectrometry, and identified a total of 104 proteins, including Qst (total spectral count = 29) (Table S2). Three enzymes that were uniquely pulled-down from the cell lysate could be directly associated with the observed metabolic changes: CoaC (phosphopantothenoylcysteine synthase/4′-phospho-N-pantothenoylcysteine decarboxylase), ThiD (phosphomethylpyrimidine kinase), and PqsD (anthraniloyl-CoA anthraniloyltransferase). Indeed, upon recombinant Qst expression in *P. aeruginosa,* the levels of the CoaC substrate 4-phosphopantothenate decreased, whereas the levels of the ThiD product 2-methyl-4-amino-5-hydroxymethylpyrimidine diphosphate increased, suggesting an increased activity of these enzymes. The third pulled-down enzyme, PqsD is a key enzyme of the PQS biosynthesis pathway, which can explain the observed decrease in PQS, HHQ, and DHQ levels (Figures 4A and S4A).

A subsequent bacterial two-hybrid experiment with Qst, PA1217, CoaC, PqsD, and ThiD consolidated the identified interactions, and revealed a complex network of mutual interactions between these proteins (Figure 5 and S6B). Nevertheless, none of the interacting proteins could be individually linked to the antibacterial activity of Qst, as expression of Qst in *P. aeruginosa* PAO1 transposon mutants of these specific genes all resulted in inhibited bacterial growth (Figure S6C).

The PQS quorum sensing system plays a key role in LUZ19 infection

A recent transcriptome analysis suggested that PQS is involved in a general host response to phage infection (Blasdel et al.,

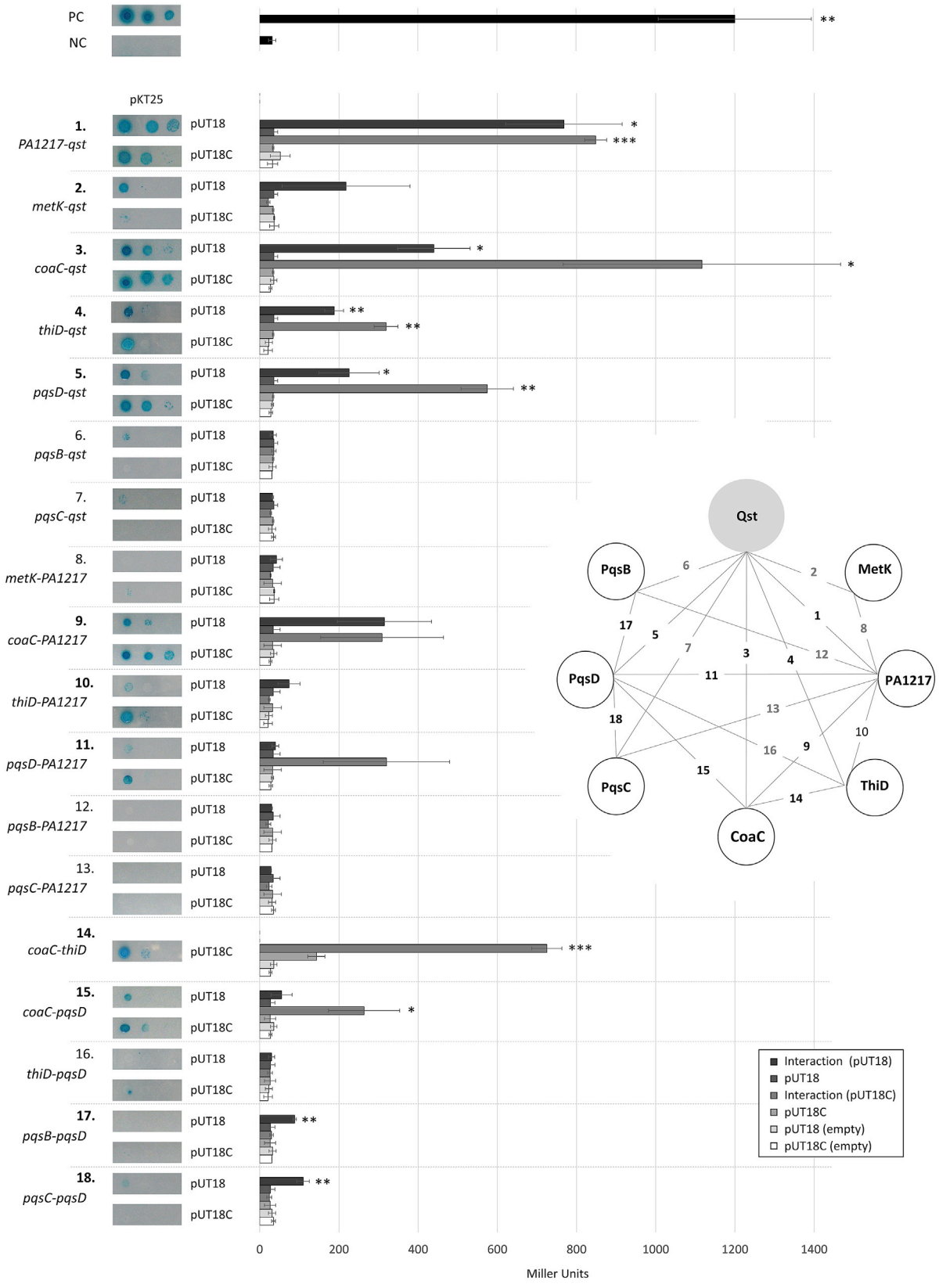

(legend on next page)

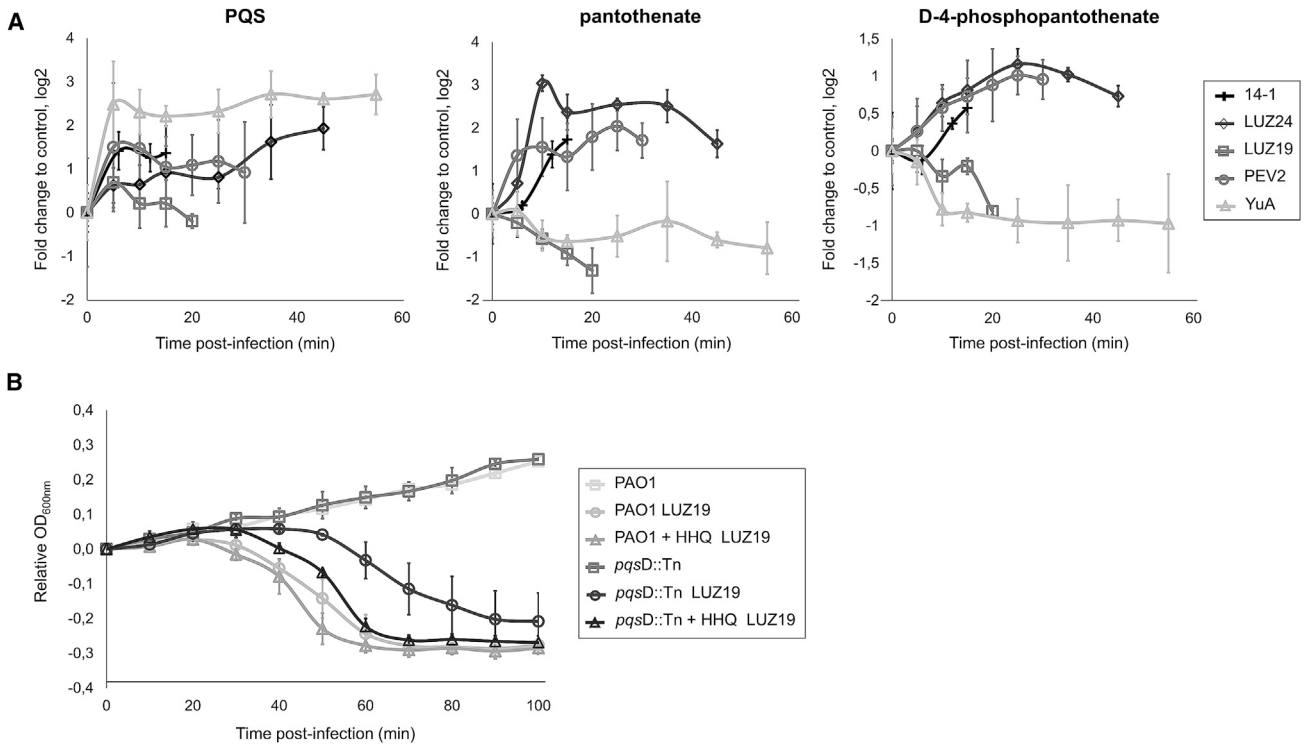

Figure 6. Role of Qst during LUZ19 infection

(A) Comparison of PQS, pantothenate and 4-phosphopantothenate metabolite levels in wild-type *P. aeruginosa* strains infected with different, unrelated clades of phages including 14-1, LUZ24, PEV2, and YuA (Ceyssens and Lavigne, 2010). The high-coverage metabolomics data of the *P. aeruginosa* phage infections were obtained from De Smet et al. (2016), who monitored the level of 518 known metabolites in *P. aeruginosa* upon phage infection. Fold changes were calculated in comparison with control samples and normalized to time 0 of infection. Error bars represent fold change SDs (n = 3). See also Table S3.

(B) Growth curves of *P. aeruginosa* PAO1 wild type and *pqsD* transposon mutant (*pqsD*::Tn) with or without LUZ19 infection, and supplemented with 100 μM HHQ. Exponentially growing *P. aeruginosa* cells (OD_{600nm} of 0.3) were infected with a multiplicity of infection of 10 and followed over time. Each data point represents the mean of the OD_{600nm}, normalized to time 0 of infection, of three replicates and error bars represent SDs (n = 3). See also Table S3 and Figure S7.

2018). To further investigate the host response, we reanalyzed a metabolomics dataset of the *Pseudomonas* phage infection process (De Smet et al., 2016) that reported that phage LUZ19 may target the PQS production at the post-transcriptional level. Indeed, upon LUZ19 infection, the metabolite levels of PQS were not increased, contrary to other *P. aeruginosa* infecting phages (Figure 6A, Table S3). We followed phage infection in transposon deletion mutants and observed that a functional PqsD is important for an efficient LUZ19 infection (Figures 6B and S7). This suggests that the interaction between Qst and PqsD has a pivotal role in host manipulation. Moreover, when the medium was supplemented with HHQ, we observed a normal LUZ19 infection in the *pqs*D transposon mutant (Figure 6B), confirming that LUZ19 harnesses this quorum sensing system during phage infection.

A comparison of the metabolomes between phages-infected *P. aeruginosa* (De Smet et al., 2016) and bacteria expressing Qst further supported the identified interaction between Qst and CoaC. Indeed, we observed substantial differences in metabolite levels of the upstream products of CoaC (pantothenate and 4-phosphopantothenate) between LUZ19 and all other tested *P. aeruginosa* infecting phages, except for phage YuA (Figure 6A).

DISCUSSION

Lytic phages contain a plethora of strategies to parasitize their host for the production of phage progeny (Roucourt and Lavigne, 2009; Wagemans et al., 2014, 2015). Here, we identified a mechanism of host-hijacking, in which the *P. aeruginosa* phage LUZ19

Figure 5. Interaction analyses of Qst and *P. aeruginosa* proteins

Bacterial two-hybrid results of Qst with PA1217, CoaC, ThiD, PqsB, PqsC, and PqsD and MetK. The diagram shows the tested combinations, in which the numbers (black: interaction; gray: no interaction) correspond with the numbers in the graph. The T25 domain is N-terminally fused to the first listed protein, the T18 domain is C- (pUT18) or N-terminally (pUT18C) fused to the second protein. Interactions were visualized by a drop test on minimal medium, and quantified by measuring the β-galactosidase activity, which are indicated in Miller Units. Non-fused T25 and T18 domains were used as a negative control, and the leucine zipper of GCN4 was used as a positive control. Error bars represent SD, and p values (compared with both controls) were calculated using the Student's t test (n = 3), *p < 0.05, **p < 0.01, ***p < 0.001. See also Figure S6B.

exploits the PQS quorum sensing system to successfully infect the host. We discovered that LUZ19 gp4 (renamed "Qst") mediates this host manipulation by directly interacting with a key PQS biosynthesis pathway enzyme, PqsD, which causes a decrease of metabolite levels of PQS and its precursor 2-heptyl-4(1H)-quinolone (HHQ). The lack of this PQS biosynthesis enzyme impairs the normal LUZ19 infection, but is restored by external supplementation of HHQ, showing the importance of quorum sensing during the viral attack. Future work will aim at unraveling the specific and targeted role of PqsD among the PQS biosynthesis enzymes during LUZ19 infection. In this regard, the recently discovered direct binding of PqsD to PQS and HHQ probes is intriguing (Baker et al., 2017; Dandela et al., 2018).

In the past years, the role of quorum sensing in adaptive regulation of phage infection has gained increasing attention. Indeed, numerous studies have demonstrated the use of quorum sensing to resist phage infection, or to switch the phage life cycle in response to environmental changes or the physiological state of the host (Erez et al., 2017; Hoyland-Kroghsbo et al., 2013, 2017; Patterson et al., 2016; Qin et al., 2017; Silpe and Bassler, 2019). For example, in *Vibrio* phage VP882, a quorum sensing receptor homolog was identified that guides the lysis-lysogeny decision (Silpe and Bassler, 2019). A potential ecologically similar mechanism was found for lambda-prophage induction in *Escherichia coli* by *P. aeruginosa* AHL quorum sensing molecules (Ghosh et al., 2009). Also recently, a quorum sensing anti-activator protein, Aqs1, inhibiting the LasR transcriptional regulator was found in the temperate *Pseudomonas* phage DMS3 (Shah et al., 2021). However, strictly lytic phages targeting quorum sensing to create a favorable infection environment has to our knowledge not yet been reported. Our previous study suggested the possibility of phage interactions with the host quorum sensing signaling (Blasdel et al., 2018; De Smet et al., 2016), which was indicated by the discrepancy between upregulated PQS biosynthesis enzymes at the transcriptional level and the reduced levels of PQS products specific to LUZ19 infection. Here we demonstrate that LUZ19 indeed directly interacts with the host quorum signaling pathway, that this interaction is mediated by the Qst enzyme, and that it is instrumental for successful phage infection.

The fact that a phage targets the PQS system is not surprising, as this system is a key regulatory hub to stress conditions, which includes phage infections. Indeed, phage-infected cells produce PQS as a stress warning signal to repel uninfected cells from the infected area (Bru et al., 2019). The PQS system is also known to decrease the cell metabolic activity during oxidative stress and to stimulate the destruction of damaged cells (Haussler and Becker, 2008). In this regard, a reduced host metabolic activity might be negative for phage progeny production. In addition, as a quorum sensing system, PQS regulates the transcription of at least 182 different genes in *P. aeruginosa*, including virulence factors, stress-related genes, and central metabolism genes (Rampioni et al., 2016). Besides quorum sensing signaling, PQS has been implicated in iron acquisition, cytotoxicity, outer-membrane vesicle biogenesis, and modulation of the host immune response (Lin et al., 2018), making it a phage target that impacts the complete host cell, which is effective for host takeover. Another hypothesis of why a phage might target the PQS system could be host energy conservation, to support phage progeny production. Indeed, PQS is one of the main regulators of virulence factor expression, which is a metabolically costly process.

Our study of Qst function revealed a functional network in *P. aeruginosa* that links quorum sensing to a previously uncharacterized NRPS pathway and to the biosynthesis of the two cofactors: pantothenate/CoA and thiamine pyrophosphate. Indeed, besides PqsD, we demonstrated that Qst interacts with PA1217, CoaC, and ThiD, of which most showed mutual interactions as well (Figure 7). Moreover, we observed that the induced expression of PA1217 abolishes the Qst-mediated metabolic changes directly linked to the other interacting partners, including the reduced PQS levels. Interestingly, the expression of PA1217 and other proteins of the same NRPS cluster are tightly regulated by quorum sensing including the PQS system via PqsE (Rampioni et al., 2016; Wagner et al., 2003), which might hint to mutual regulation. The impact of Qst on multiple metabolic pathways might explain the growth-inhibitory effect of Qst on *P. aeruginosa* cells, which is in line with other examples of small phage proteins targeting multiple host proteins to enable efficient infection (Häuser et al., 2012).

Despite the clear evidence for the identified interactions and their biological impact provided in this study, the precise molecular function of Qst remains to be elucidated. Since Qst, PA1217, and PqsD are all linked to acyltransferase activity, for which CoaC supplies the cofactor CoA and 4-phosphopantetheine (prosthetic group in acyl carrier proteins) (Kanehisa and Goto, 2000), we hypothesize that the binary interactions support an efficient channeling of metabolites, and that Qst imposes an additional level of regulation to these enzymes through post-translational modification or direct protein-protein interactions. The interaction between Qst and the catalytic part of PA1217 indicates a potential influence of Qst on the enzymatic activity or specificity of its targets. The direct effect of Qst on the substrate and product levels of CoaC and ThiD, respectively, suggests a phage-mediated overactivation of these enzymes. Interestingly, the interactions CoaC-PqsD and CoaC-ThiD have been predicted using a machine learning-based integrative approach (Zhang et al., 2012). The fact that ThiD interacts with neither PA1217 nor PqsD is consistent with the interaction predictions, since no relationship between these enzymes is reported.

Taken together, in this study we uncovered a phage-based mechanism of host-hijacking to support phage infection via quorum sensing modulation. Our results emphasize the importance and multilevel role of quorum sensing during viral attack. The fact that Qst targets PqsD is even more intriguing, as this enzyme catalyzes a key step in HHQ biosynthesis, which makes it a widely studied anti-virulence and anti-biofilm target to combat *P. aeruginosa* infections (Storz et al., 2012; Weidel et al., 2013; Zhou and Ma, 2017). Moreover, the Qst interaction partners CoaC and ThiD are studied for their potential as antibacterial drug targets (Du et al., 2011; O'Toole and Cygler, 2003). Therefore, Qst could be a promising tool in the battle against antibiotic resistant *P. aeruginosa*.

Limitations of the study

This study explores one of the early genes of a bacteriophage infecting *P. aeruginosa*. Although an integrative approach was

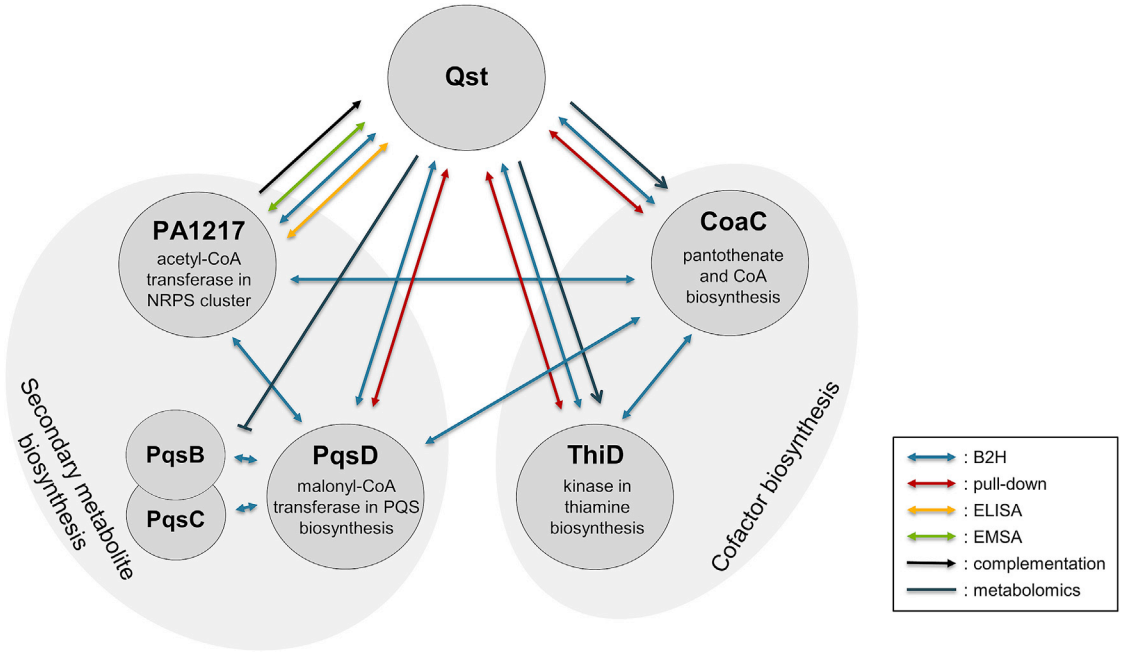

Figure 7. Schematic overview of the influence of Qst on *P. aeruginosa*

Four interaction partners of Qst were identified with high confidence using metabolomics and interactomics. Two interaction partners are involved in cofactor biosynthetic processes (enzymes CoaC and ThiD), and two are part of secondary metabolite biosynthesis pathways: (1) one the well-known quorum sensing molecule PQS (PqsD) and (2) one of a predicted non-ribosomal peptide (PA1217 from the PA1221 cluster). The protein of the latter pathway, PA1217, is tightly regulated by quorum sensing and is able to neutralize the antibacterial effect of Qst (complementation). Recombinant expression of Qst in *P. aeruginosa* increases and decreases respectively the metabolite levels of the substrate of CoaC and the product of ThiD, suggesting that Qst mediates overactivation of these enzymes. Moreover, the PQS quorum sensing system of *P. aeruginosa* is modulated by Qst, that directly interacts with PqsD resulting in decreased metabolite levels of its downstream products, including HHQ. The four protein-protein interaction techniques applied in this research were bacterial two-hybrid, pull-down, ELISA and electrophoretic mobility shift assay, and are marked in blue, red, yellow, and green, respectively.

used, the study of this phage protein was focused on an inducible expression system in the absence of the phage. A gene knockout phage would allow assessment of its effects in the context of phage infection. However, genome manipulation of strictly lytic phages remains challenging, as their genome does not integrate into the bacterial chromosome, remaining a short time frame for engineering. Therefore, the development of an efficient and reproducible gene-editing tool for the engineering of virulent *Pseudomonas* phage genomes would greatly aid phage-host interaction research.

STAR★METHODS

Detailed methods are provided in the online version of this paper and include the following:

SUPPLEMENTAL INFORMATION

Supplemental information can be found online at https://doi.org/10.1016/j.celrep.2022.110372.

ACKNOWLEDGMENTS

We thank Prof. Dirk De Vos (Center for Surface Chemistry and Catalysis, KU Leuven, Belgium) for use of the NMR facilities and Erik Royackers (Hasselt University, Belgium) for the technical support in mass spectrometry analysis. This research was supported by the KU Leuven project GOA "Phage Biosystems" (GOA/15/006) and the C1 project 'ACES' (C16/20/001).

AUTHOR CONTRIBUTIONS

J.W., I.S., P-J.C., and H.H. carried out the toxicity screenings. J.D. and H.H. prepared the metabolomics samples, and M.Z.-K, M.Z., and U.S. analyzed the metabolomics data. M.L., M.V., and H.H. carried out the bacterial two-hybrid analysis. L.M. carried out the ^{1}H-NMR analysis. J-P.N. carried out the mass spectrometry analysis. H.H., A.A., and R.L. designed the experiments. H.H. wrote the manuscript and all authors commented on the manuscript.

DECLARATION OF INTERESTS

The authors declare no competing interests.

Received: June 1, 2020
Revised: July 29, 2021
Accepted: January 21, 2022
Published: February 15, 2022

REFERENCES

Adriaenssens, E.M., Sullivan, M.B., Knezevic, P., van Zyl, L.J., Sarkar, B.L., Dutilh, B.E., Alfenas-Zerbini, P., Łobocka, M., Tong, Y., Brister, J.R., et al. (2020). Taxonomy of prokaryotic viruses: 2018-2019 update from the ICTV bacterial and archaeal viruses subcommittee. Arch. Virol. *165*, 1253–1260. https://doi.org/10.1007/s00705-020-04577-8.

Altschul, S.F., Gish, W., Miller, W., Myers, E.W., and Lipman, D.J. (1990). Basic local alignment search tool. J. Mol. Biol. *215*, 403–410. https://doi.org/10.1016/S0022-2836(05)80360-2.

Baker, Y.R., Hodgkinson, J.T., Florea, B.I., Alza, E., Galloway, W.R.J.D., Grimm, L., Geddis, S.M., Overkleeft, H.S., Welch, M., and Spring, D.R. (2017). Identification of new quorum sensing autoinducer binding partners in *Pseudomonas aeruginosa* using photoaffinity probes. Chem. Sci. *8*, 7403–7411. https://doi.org/10.1039/c7sc01270e.

Blasdel, B.G., Ceyssens, P.-J., Chevallereau, A., Debarbieux, L., and Lavigne, R. (2018). Comparative transcriptomics reveals a conserved Bacterial Adaptive Phage Response (BAPR) to viral predation. bioRxiv, 248849. https://doi.org/10.1101/248849.

Bru, J.-L., Rawson, B., Trinh, C., Whiteson, K., Hoyland-Kroghsbo, N.M., and Siryaporn, A. (2019). PQS produced by the *Pseudomonas aeruginosa* stress response repels swarms away from bacteriophage and antibiotics. J. Bacteriol. *201*, e00383–19. https://doi.org/10.1128/JB.00383-19.

Cenens, W., Mebrhatu, M.T., Makumi, A., Ceyssens, P.-J., Lavigne, R., Van Houdt, R., Taddei, F., and Aertsen, A. (2013). Expression of a novel P22 ORFan gene reveals the phage carrier state in *Salmonella typhimurium*. PLoS Genet. *9*, e1003269. https://doi.org/10.1371/journal.pgen.1003269.

Ceyssens, P.-J., and Lavigne, R. (2010). Bacteriophages of *Pseudomonas*. Future Microbiol. *5*, 1041–1055. https://doi.org/10.2217/fmb.10.66.

Choi, K.-H., Gaynor, J.B., White, K.G., Lopez, C., Bosio, C.M., Karkhoff-Schweizer, R.R., and Schweizer, H.P. (2005). A Tn7-based broad-range bacterial cloning and expression system. Nat. Methods *2*, 443–448. https://doi.org/10.1038/nmeth765.

Choi, K.-H., Kumar, A., and Schweizer, H.P. (2006). A 10-min method for preparation of highly electrocompetent *Pseudomonas aeruginosa* cells: application for DNA fragment transfer between chromosomes and plasmid transformation. J. Microbiol. Methods *64*, 391–397. https://doi.org/10.1016/j.mimet.2005.06.001.

Chugani, S., Kim, B.S., Phattarasukol, S., Brittnacher, M.J., Choi, S.H., Harwood, C.S., and Greenberg, E.P. (2012). Strain-dependent diversity in the *Pseudomonas aeruginosa* quorum-sensing regulon. Proc. Natl. Acad. Sci. U. S. A. *109*, 2823–2831. https://doi.org/10.1073/pnas.1214128109.

Dandela, R., Mantin, D., Cravatt, B.F., Rayo, J., and Meijler, M.M. (2018). Proteome-wide mapping of PQS-interacting proteins in *Pseudomonas aeruginosa*. Chem. Sci. *9*, 2290–2294. https://doi.org/10.1039/c7sc04287f.

D'Argenio, D.A., Calfee, M.W., Rainey, P.B., and Pesci, E.C. (2002). Autolysis and autoaggregation in *Pseudomonas aeruginosa* colony morphology mutants. J. Bacteriol. *184*, 6481–6489. https://doi.org/10.1128/JB.184.23.6481-6489.2002.

de Carvalho, L.P.S., and Blanchard, J.S. (2006). Kinetic and chemical mechanism of alpha-isopropylmalate synthase from *Mycobacterium tuberculosis*. Biochemistry *45*, 8988–8999. https://doi.org/10.1021/bi0606602.

De Smet, J., Hendrix, H., Blasdel, B.G., Danis-Wlodarczyk, K., and Lavigne, R. (2017). *Pseudomonas* predators: understanding and exploiting phage-host interactions. Nat. Rev. Microbiol. *15*, 517–530. https://doi.org/10.1038/nrmicro.2017.61.

De Smet, J., Zimmermann, M., Kogadeeva, M., Ceyssens, P.-J., Vermaelen, W., Blasdel, B., Bin Jang, H., Sauer, U., and Lavigne, R. (2016). High coverage metabolomics analysis reveals phage-specific alterations to *Pseudomonas aeruginosa* physiology during infection. ISME J. *10*, 1823–1835. https://doi.org/10.1038/ismej.2016.3.

Du, Q., Wang, H., and Xie, J. (2011). Thiamin (vitamin B1) biosynthesis and regulation: a rich source of antimicrobial drug targets? Int. J. Biol. Sci. *7*, 41–52. https://doi.org/10.7150/ijbs.7.41.

Dubern, J.-F., and Diggle, S.P. (2008). Quorum sensing by 2-alkyl-4-quinolones in *Pseudomonas aeruginosa* and other bacterial species. Mol. Biosyst. *4*, 882–888. https://doi.org/10.1039/b803796p.

Enos-Berlage, J.L., and Downs, D.M. (1997). Mutations in sdh (succinate dehydrogenase genes) alter the thiamine requirement of *Salmonella typhimurium*. J. Bacteriol. *179*, 3989–3996.

Erez, Z., Steinberger-Levy, I., Shamir, M., Doron, S., Stokar-Avihail, A., Peleg, Y., Melamed, S., Leavitt, A., Savidor, A., Albeck, S., et al. (2017). Communication between viruses guides lysis-lysogeny decisions. Nature *541*, 488–493. https://doi.org/10.1038/nature21049.

Fletcher, M.P., Diggle, S.P., Cámara, M., and Williams, P. (2007). Biosensor-based assays for PQS, HHQ and related 2-alkyl-4-quinolone quorum sensing signal molecules. Nat. Protoc. *2*, 1254–1262. https://doi.org/10.1038/nprot.2007.158.

Gambello, M.J., and Iglewski, B.H. (1991). Cloning and characterization of the *Pseudomonas aeruginosa* lasR gene, a transcriptional activator of elastase expression. J. Bacteriol. *173*, 3000–3009. https://doi.org/10.1128/jb.173.9.3000-3009.1991.

Ghosh, D., Roy, K., Williamson, K.E., Srinivasiah, S., Wommack, K.E., and Radosevich, M. (2009). Acyl-homoserine lactones can induce virus production in lysogenic bacteria: an alternative paradigm for prophage induction. Appl. Environ. Microbiol. *75*, 7142–7152.

Gulick, A.M. (2017). Nonribosomal peptide synthetase biosynthetic clusters of ESKAPE pathogens. Nat. Prod. Rep. *34*, 981–1009. https://doi.org/10.1039/c7np00029d.

Häuser, R., Blasche, S., Dokland, T., Haggard-Ljungquist, E., von Brunn, A., Salas, M., Casjens, S., Molineux, I., and Uetz, P. (2012). Bacteriophage protein-protein interactions. Adv. Virus Res. *83*, 219–298. https://doi.org/10.1016/B978-0-12-394438-2.00006-2.

Haussler, S., and Becker, T. (2008). The *Pseudomonas* quinolone signal (PQS) balances life and death in *Pseudomonas aeruginosa* populations. PLoS Pathog. *4*, e1000166. https://doi.org/10.1371/journal.ppat.1000166.

Hazra, A., Chatterjee, A., Chatterjee, D., Hilmey, D.G., Sanders, J.M., Hanes, J.W., Krishnamoorthy, K., McCulloch, K.M., Waitner, M.J., O'Leary, S., et al. (2009). In Coenzyme and Prosthetic Group Biosynthesis in Encyclopedia of Microbiology, Third Edition, M. Schaechter, ed. (Oxford, UK: Academic Press), pp. 79–88. https://doi.org/10.1016/B978-012373944-5.00069-9.

Heeb, S., Blumer, C., and Haas, D. (2002). Regulatory RNA as mediator in GacA/RsmA-dependent global control of exoproduct formation in *Pseudomonas fluorescens* CHA0. J. Bacteriol. *184*, 1046–1056. https://doi.org/10.1128/jb.184.4.1046-1056.2002.

Held, K., Ramage, E., Jacobs, M., Gallagher, L., and Manoil, C. (2012). Sequence-verified two-allele transposon mutant library for *Pseudomonas*

aeruginosa PAO1. J. Bacteriol. *194*, 6387–6389. https://doi.org/10.1128/JB.01479-12.

Hendrix, H., Staes, I., Aertsen, A., and Wagemans, J. (2019). Screening for growth-Inhibitory ORFans in *Pseudomonas aeruginosa*-infecting bacteriophages. Methods Mol. Biol. *1898*, 147–162. https://doi.org/10.1007/978-1-4939-8940-9_12.

Hoyland-Kroghsbo, N.M., Maerkedahl, R.B., and Svenningsen, S.L. (2013). A quorum-sensing-induced bacteriophage defense mechanism. mBio *4*, e00362–12. https://doi.org/10.1128/mBio.00362-12.

Hoyland-Kroghsbo, N.M., Paczkowski, J., Mukherjee, S., Broniewski, J., Westra, E., Bondy-Denomy, J., and Bassler, B.L. (2017). Quorum sensing controls the *Pseudomonas aeruginosa* CRISPR-Cas adaptive immune system. Proc. Natl. Acad. Sci. U. S. A. *114*, 131–135. https://doi.org/10.1073/pnas.1617415113.

Hurwitz, B.L., Hallam, S.J., and Sullivan, M.B. (2013). Metabolic reprogramming by viruses in the sunlit and dark ocean. Genome Biol. *14*, R123. https://doi.org/10.1186/gb-2013-14-11-r123.

Jenul, C., Sieber, S., Daeppen, C., Mathew, A., Lardi, M., Pessi, G., Hoepfner, D., Neuburger, M., Linden, A., Gademann, K., and Eberl, L. (2018). Biosynthesis of fragin is controlled by a novel quorum sensing signal. Nat. Commun. *9*, 1297. https://doi.org/10.1038/s41467-018-03690-2.

Kanehisa, M., and Goto, S. (2000). KEGG: kyoto encyclopedia of genes and genomes. Nucleic Acids Res. *28*, 27–30. https://doi.org/10.1093/nar/28.1.27.

Lammens, E., Ceyssens, P.-J., Voet, M., Hertveldt, K., Lavigne, R., and Volckaert, G. (2009). Representational difference analysis (RDA) of bacteriophage genomes. J. Microbiol. Methods *77*, 207–213. https://doi.org/10.1016/j.mimet.2009.02.0.

Lavigne, R., Lecoutere, E., Wagemans, J., Cenens, W., Aertsen, A., Schoofs, L., Landuyt, B., Paeshuyse, J., Scheer, M., Schobert, M., and Ceyssens, P.-J. (2013). A multifaceted study of *Pseudomonas aeruginosa* shutdown by virulent podovirus LUZ19. mBio *4*, e00061–13. https://doi.org/10.1128/mBio.00061-13.

Lin, J., Cheng, J., Wang, Y., and Shen, X. (2018). The *Pseudomonas* Quinolone Signal (PQS): not just for quorum sensing anymore. Front. Cell. Infect. Microbiol. *8*, 230. https://doi.org/10.3389/fcimb.2018.00230.

McDaniel, L.D., Young, E., Delaney, J., Ruhnau, F., Ritchie, K.B., and Paul, J.H. (2010). High frequency of horizontal gene transfer in the oceans. Science *330*, 50. https://doi.org/10.1126/science.1192243.

Mitchell, C.A., Shi, C., Aldrich, C.C., and Gulick, A.M. (2012). Structure of PA1221, a nonribosomal peptide synthetase containing adenylation and peptidyl carrier protein domains. Biochemistry *51*, 3252–3263. https://doi.org/10.1021/bi300112e.

O'Toole, N., and Cygler, M. (2003). The final player in the coenzyme A biosynthetic pathway. Structure *11*, 899–900. https://doi.org/10.1016/S0969-2126(03)00161-8.

Patterson, A.G., Jackson, S.A., Taylor, C., Evans, G.B., Salmond, G.P.C., Przybilski, R., Staals, R.H.J., and Fineran, P.C. (2016). Quorum sensing controls adaptive immunity through the regulation of multiple CRISPR-Cas systems. Mol. Cell *64*, 1102–1108. https://doi.org/10.1016/j.molcel.2016.11.012.

Pesci, E.C., Pearson, J.P., Seed, P.C., and Iglewski, B.H. (1997). Regulation of las and rhl quorum sensing in *Pseudomonas aeruginosa*. J. Bacteriol. *179*, 3127–3132. https://doi.org/10.1128/jb.179.10.3127-3132.1997.

Qin, X., Sun, Q., Yang, B., Pan, X., He, Y., and Yang, H. (2017). Quorum sensing influences phage infection efficiency via affecting cell population and physiological state. J. Basic Microbiol. *57*, 162–170. https://doi.org/10.1002/jobm.201600510.

Qiu, D., Damron, F.H., Mima, T., Schweizer, H.P., and Yu, H.D. (2008). PBAD-based shuttle vectors for functional analysis of toxic and highly regulated genes in *Pseudomonas* and *Burkholderia* spp. and other bacteria. Appl. Environ. Microbiol. *74*, 7422–7426. https://doi.org/10.1128/AEM.01369-08.

Rampioni, G., Falcone, M., Heeb, S., Frangipani, E., Fletcher, M.P., Dubern, J.-F., Visca, P., Leoni, L., Camara, M., and Williams, P. (2016). Unravelling the genome-wide contributions of specific 2-alkyl-4-quinolones and PqsE to quorum sensing in *Pseudomonas aeruginosa*. PLoS Pathog. *12*, e1006029. https://doi.org/10.1371/journal.ppat.1006029.

Roucourt, B., and Lavigne, R. (2009). The role of interactions between phage and bacterial proteins within the infected cell: a diverse and puzzling interactome. Environ. Microbiol. *11*, 2789–2805. https://doi.org/10.1111/j.1462-2920.2009.02029.x.

Roucourt, B., Minnebo, N., Augustijns, P., Hertveldt, K., Volckaert, G., and Lavigne, R. (2009). Biochemical characterization of malate synthase G of *P. aeruginosa*. BMC Biochem. *10*, 20. https://doi.org/10.1186/1471-2091-10-20.

Rouhiainen, L., Jokela, J., Fewer, D.P., Urmann, M., and Sivonen, K. (2010). Two alternative starter modules for the non-ribosomal biosynthesis of specific anabaenopeptin variants in *Anabaena* (Cyanobacteria). Chem. Biol. *17*, 265–273. https://doi.org/10.1016/j.chembiol.2010.01.017.

Samson, J.E., Magadan, A.H., Sabri, M., and Moineau, S. (2013). Revenge of the phages: defeating bacterial defences. Nat. Rev. Microbiol. *11*, 675–687. https://doi.org/10.1038/nrmicro3096.

Schindelin, J., Arganda-Carreras, I., Frise, E., Kaynig, V., Longair, M., Pietzsch, T., Preibisch, S., Rueden, C., Saalfeld, S., Schmid, B., et al. (2012). Fiji: an open-source platform for biological-image analysis. Nat. Methods *9*, 676–682. https://doi.org/10.1038/nmeth.2019.

Schuster, M., Lostroh, C.P., Ogi, T., and Greenberg, E.P. (2003). Identification, timing, and signal specificity of *Pseudomonas aeruginosa* quorum-controlled genes: a transcriptome analysis. J. Bacteriol. *185*, 2066–2079. https://doi.org/10.1128/jb.185.7.2066-2079.2003.

Shah, M., Taylor, V.L., Bona, D., Tsao, Y., Stanley, S.Y., Pimentel-Elardo, S.M., McCallum, M., Bondy-Denomy, J., Howell, P.L., Nodwell, J.R., et al. (2021). A phage-encoded anti-activator inhibits quorum sensing in *Pseudomonas aeruginosa*. Mol. Cell. *81*, 571–583. https://doi.org/10.1016/j.molcel.2020.12.011.

Silpe, J.E., and Bassler, B.L. (2019). A host-produced quorum-sensing autoinducer controls a phage lysis-lysogeny decision. Cell *176*, 268–280.e13. https://doi.org/10.1016/j.cell.2018.10.059.

Spalding, M.D., and Prigge, S.T. (2010). Lipoic acid metabolism in microbial pathogens. Microbiol. Mol. Biol. Rev. *74*, 200–228. https://doi.org/10.1128/MMBR.00008-10.

Storz, M.P., Maurer, C.K., Zimmer, C., Wagner, N., Brengel, C., de Jong, J.C., Lucas, S., Musken, M., Haussler, S., Steinbach, A., and Hartmann, R.W. (2012). Validation of PqsD as an anti-biofilm target in *Pseudomonas aeruginosa* by development of small-molecule inhibitors. J. Am. Chem. Soc. *134*, 16143–16146. https://doi.org/10.1021/ja3072397.

Stover, C.K., Pham, X.Q., Erwin, A.L., Mizoguchi, S.D., Warrener, P., Hickey, M.J., Brinkman, F.S., Hufnagle, W.O., Kowalik, D.J., Lagrou, M., et al. (2000). Complete genome sequence of *Pseudomonas* aeruginosa PAO1, an opportunistic pathogen. Nature *406*, 959–964. https://doi.org/10.1038/35023079.

Suttle, C.A. (2007). Marine viruses–major players in the global ecosystem. Nat. Rev. Microbiol. *5*, 801–812. https://doi.org/10.1038/nrmicro1750.

Thompson, L.R., Zeng, Q., Kelly, L., Huang, K.H., Singer, A.U., Stubbe, J., and Chisholm, S.W. (2011). Phage auxiliary metabolic genes and the redirection of cyanobacterial host carbon metabolism. Proc. Natl. Acad. Sci. U. S. A. *108*, 757–764. https://doi.org/10.1073/pnas.1102164108.

Van den Bossche, A., Ceyssens, P.-J., De Smet, J., Hendrix, H., Bellon, H., Leimer, N., Wagemans, J., Delattre, A.-S., Cenens, W., Aertsen, et al. (2014). Systematic identification of hypothetical bacteriophage proteins targeting key protein complexes of *Pseudomonas aeruginosa*. J. Proteome Res. *13*, 4446–4456. https://doi.org/10.1021/pr500796n.

Van den Bossche, A., Hardwick, S.W., Ceyssens, P.-J., Hendrix, H., Voet, M., Dendooven, T., Bandyra, K.J., De Maeyer, M., Aertsen, A., Noben, J.-P., et al. (2016). Structural elucidation of a novel mechanism for the bacteriophage-based inhibition of the RNA degradosome. Elife *5*, e16413. https://doi.org/10.7554/eLife.16413.

Van Houdt, R., Aertsen, A., Jansen, A., Quintana, A.L., and Michiels, C.W. (2004). Biofilm formation and cell-to-cell signalling in Gram-negative bacteria

isolated from a food processing environment. J. Appl. Microbiol. *96*, 177–184. https://doi.org/10.1046/j.1365-2672.2003.02131.x.

Wagemans, J., Blasdel, B.G., Van den Bossche, A., Uytterhoeven, B., De Smet, J., Paeshuyse, J., Cenens, W., Aertsen, A., Uetz, P., Delattre, A.-S., et al. (2014). Functional elucidation of antibacterial phage ORFans targeting *Pseudomonas aeruginosa*. Cell. Microbiol. *16*, 1822–1835. https://doi.org/10.1111/cmi.12330.

Wagemans, J., Delattre, A.-S., Uytterhoeven, B., De Smet, J., Cenens, W., Aertsen, A., Ceyssens, P.-J., and Lavigne, R. (2015). Antibacterial phage ORFans of *Pseudomonas aeruginosa* phage LUZ24 reveal a novel MvaT inhibiting protein. Front. Microbiol. *6*, 1242. https://doi.org/10.3389/fmicb.2015.01242.

Wagner, V.E., Bushnell, D., Passador, L., Brooks, A.I., and Iglewski, B. (2003). Microarray analysis of *Pseudomonas aeruginosa* quorum-sensing regulons: effects of growth phase and environment. J. Bacteriol. *185*, 2080–2095.

Weidel, E., de Jong, J.C., Brengel, C., Storz, M.P., Braunshausen, A., Negri, M., Plaza, A., Steinbach, A., Muller, R., and Hartmann, R.W. (2013). Structure optimization of 2-benzamidobenzoic acids as PqsD inhibitors for *Pseudomonas aeruginosa* infections and elucidation of binding mode by SPR, STD NMR, and molecular docking. J. Med. Chem. *56*, 6146–6155. https://doi.org/10.1021/jm4006302.

Williams, P., and Camara, M. (2009). Quorum sensing and environmental adaptation in *Pseudomonas aeruginosa*: a tale of regulatory networks and multifunctional signal molecules. Curr. Opin. Microbiol. *12*, 182–191. https://doi.org/10.1016/j.mib.2009.01.005.

Winsor, G.L., Griffiths, E.J., Lo, R., Dhillon, B.K., Shay, J.A., and Brinkman, F.S.L. (2016). Enhanced annotations and features for comparing thousands of *Pseudomonas* genomes in the *Pseudomonas* genome database. Nucleic Acids Res. *44*, 646–653. https://doi.org/10.1093/nar/gkv1227.

Zhang, M., Su, S., Bhatnagar, R.K., Hassett, D.J., and Lu, L.J. (2012). Prediction and analysis of the protein interactome in *Pseudomonas aeruginosa* to enable network-based drug target selection. PLoS One *7*, e41202. https://doi.org/10.1371/journal.pone.0041202.

Zhang, X., and Bremer, H. (1995). Control of the *Escherichia coli* rrnB P1 promoter strength by ppGpp. J. Biol. Chem. *270*, 11181–11189. https://doi.org/10.1074/jbc.270.19.11181.

Zhou, Z., and Ma, S. (2017). Recent advances in the discovery of PqsD Inhibitors as antimicrobial agents. ChemMedChem *12*, 420–425. https://doi.org/10.1002/cmdc.201700015.

STAR★METHODS

KEY RESOURCES TABLE

REAGENT or RESOURCE	SOURCE	IDENTIFIER
Antibodies		
monoclonal Anti-His antibody	Sigma-Aldrich	Cat# H1029-; RRID: AB_260015
Anti-Mouse IgG antibody conjugated to HRP	Promega	Cat# W4021; RRID: AB_430834
Bacterial and virus strains		
E. coli TOP10	Thermo Fisher Scientific	Cat#C404010
E. coli BL21(DE3)	Thermo Fisher Scientific	Cat#C606003
E. coli BTH101	Euromedex	Cat#EUK001
P. aeruginosa PAO1	Stover et al., 2000	N/A
P. aeruginosa PAO1-R1	Gambello and Iglewski, 1991	N/A
P. aeruginosa PAO1 *pqsA*::Tn	Held et al., 2012	UWGC: PW2799
P. aeruginosa PAO1 *pqsB*::Tn	Held et al., 2012	UWGC: PW2800
P. aeruginosa PAO1 *pqsC*::Tn	Held et al., 2012	UWGC: PW2803
P. aeruginosa PAO1 *pqsD*::Tn	Held et al., 2012	UWGC: PW2805
P. aeruginosa PAO1 *pqsE*::Tn	Held et al., 2012	UWGC: PW2806
P. aeruginosa PAO1 *pqsH*::Tn	Held et al., 2012	UWGC: PW5343
P. aeruginosa PAO1 *pqsL*::Tn	Held et al., 2012	UWGC: PW8105
P. aeruginosa PAO1 *thiD*::Tn	Held et al., 2012	UWGC: PW7728
P. aeruginosa PAO1 PA1217::Tn	Held et al., 2012	UWGC: PW3197
P. aeruginosa PAO1 mini-Tn7T-LUZ19_*qst*	This paper	N/A
P. aeruginosa PAO1 *pqsD*::Tn, mini-Tn7T-LUZ19_*qst*	This paper	N/A
P. aeruginosa PAO1 *thiD*::Tn, mini-Tn7T-LUZ19_*qst*	This paper	N/A
P. aeruginosa PAO1 PA1217::Tn, mini-Tn7T-LUZ19_*qst*	This paper	N/A
Pseudomonas phage LUZ19	Lammens et al., 2009	NC_010326
Chemicals, peptides, and recombinant proteins		
Purified protein: LUZ19 gp4/Qst-His	This paper	N/A
Purified protein: PA1217-GST	This paper	N/A
Purified protein PAO1 LeuA-GST	This paper	N/A
1-Step Slow TMB-ELISA substrate	Thermo Fisher Scientific	Cat#34024
Critical commercial assays		
BACTH System kit	Euromedex	Cat#EUK001
Gateway Vector Conversion System	Thermo Fisher Scientific	Cat#11828-029
pENTR/SD/D-TOPO cloning kit	Thermo Fisher Scientific	Cat# K242020
LR Clonase Enzyme mix	Thermo Fisher Scientific	Cat#11791019
Oligonucleotides		
See Table S4		N/A
Recombinant DNA		
pUC18-mini-Tn7T-Lac	Choi et al., 2005	Addgene: #63121
pUC18-mini-Tn7T-Lac-LUZ19_*qst*	This paper	N/A
pTNS2	Choi et al., 2005	Addgene: #64968
pGEX-6P-1	Cytiva	Cat#28954648
pGEX-6P-1-PA1217	This paper	N/A
pGEX-6P-1-*leuA*	This paper	N/A
pEXP5-TOPO/CT	Thermo Fisher Scientific	Cat#V96006
pEXP5-TOPO/CT-LUZ19_*qst*	This paper	N/A
pHERD20T	Qiu et al., 2008	GenBank: EU603324.1

(*Continued on next page*)

Continued

REAGENT or RESOURCE	SOURCE	IDENTIFIER
pHERD20T–*P. aeruginosa* PAO1 genome library	This paper	N/A
pME6032	Heeb et al., 2002	N/A
pME6032–PA1216	This paper	N/A
pME6032–PA1217	This paper	N/A
pN-25	Euromedex	Cat#EUK001
pN-25 derivatives (see Figure S2)	This paper	N/A
pKT25	Euromedex	Cat#EUK001
pKT25 derivatives (See Figure 5)	This paper	N/A
pUT18	Euromedex	Cat#EUK001
pUT18 derivatives (See Figure 5)	This paper	N/A
pUT18C	Euromedex	Cat#EUK001
pUT18C derivatives (See Figure 5)	This paper	N/A
Software and algorithms		
NIS-Elements AR 3.2 software	Nikon	https://www.microscope.healthcare.nikon.com/
Open source software Fiji (i.e., ImageJ)	Schindelin et al., 2012	https://fiji.sc/
Sequencher	Gene Codes	https://www.genecodes.com/free-download
Proteome Discoverer v.1.3 Sequest v.1.4.0.288 Mascot v.4.4.1.1.	Thermo Fisher Scientific Thermo Fisher Scientific Matrix Science	https://thermo-proteome-discoverer.software.informer.com/1.3/
Matlab Page package	MathWorks	http://www.mathworks.com/matlabcentral/fileexchange/14419-perform-page-test?focused=6141676&tab=function
Other		
1 mL HisTrap HP column	Cytiva	Cat#17524701
GSTrap HP column	Cytiva	Cat#17528202
Ni-NTA Superflow beads	QIAGEN	Cat#30410
1 mL Polypropylene column	QIAGEN	Cat#34924
Pierce™ Anti-GST Coated Clear Strip Plates	Thermo Fisher Scientific	Cat#15144
Silica 60 F254 TLC plate	Merck	Cat# 1055700001

RESOURCE AVAILABILITY

Lead contact

Further information and requests for resources and reagents should be directed to and will be fulfilled by the lead contact, Prof. Rob Lavigne (rob.lavigne@kuleuven.be).

Materials availability

Plasmids and strains generated in this study are available at the Laboratory of Gene Technology, KU Leuven upon request. Contact Prof. Rob Lavigne (rob.lavigne@kuleuven.be) for any further information.

Data and code availability

- All data reported in this paper will be shared by the lead contact upon request.
- This paper does not report original code.
- Any additional information required to reanalyze the data reported in this paper is available from the lead contact (rob.lavigne@kuleuven.be) upon request.

EXPERIMENTAL MODEL AND SUBJECT DETAILS

Bacterial strains

Pseudomonas aeruginosa PAO1 and derivatives were used in this study (Stover et al., 2000). Strain PAO1-R1, a lasR^{-}lasI^{-} mutant containing the pTS400 plasmid (*lasB′-lacZ* translational fusion), was used for the bioassay (Gambello and Iglewski, 1991). Transposon deletion mutants were ordered from the *P. aeruginosa* mutant library (Held et al., 2012): PW2799, PW2800, PW2803, PW2805, PW2806, PW5343, PW8105, PW7728, PW3198. *P. aeruginosa* PAO1 strains with single-copy integration of the phage gene under a *lac* promotor

into the bacterial genome were made using the Gateway cloning system (Thermo Fisher Scientific), as described previously (Hendrix et al., 2019). Three *Escherichia coli* strains were used: *E. coli* TOP10 (Thermo Fisher Scientific) for cloning procedures, *E. coli* BTH101 (Euromedex, Souffelweyersheim, F) for Bacterial two-hybrid assays and *E. coli* BL21(DE3) (Thermo Fisher Scientific) for recombinant protein expression. All these microbes can be cultivated in LB broth at a temperature of 37°C.

Bacteriophages

Pseudomonas phage LUZ19 was amplified on *P. aeruginosa* PAO1 using the soft agar overlay method, followed by PEG8000 precipitation (Lavigne et al., 2013), and stored in phage buffer (10 mM Tris pH 7.5, 10 mM $MgSO_4$, 150 mM NaCl) at 4°C. The number of phages was estimated by plating a dilution series of the phage with the soft agar overlay method and counting of the number of plaque forming units (pfu).

METHOD DETAILS

Genome fragment library construction

A *P. aeruginosa* PAO1 fragment library was constructed by ligating genomic DNA fragments into the pHERD20T vector (Qiu et al., 2008). For this, restriction enzymes AluI and RsaI (Thermo Scientific, Waltham, MA) were applied to fragment 37.5 μg purified genomic DNA, and restriction enzyme SmaI (Thermo Scientific) was used to digest 3 μg pHERD20T vector according the manufacturer's protocol. The fragments with lengths between 1.5 kbp and 4 kbp were isolated using gel extraction and concentrated by ethanol precipitation. The digested vector, on the other hand, was treated with alkaline phosphatase FastAP (Thermo Scientific). The ligation reaction mixture, with a total volume of 20 μL, contained a three-fold excess of DNA fragments compared to the pHERD20T vector (50 ng), 1 μL T4 DNA ligase, 2 μL T4 buffer and 2 μL 50% PEG4000 (Merck, Kenilworth, NJ). After incubation, the entire library was transformed to chemically competent *E. coli* TOP10 cells and the number of transformants was determined.

Complementation assays

The *P. aeruginosa* PAO1 genome fragment library, containing random fragments ranging from 1.5 to 4 kbp inserted in a pHERD20T vector under control of a p*BAD* promotor, was electroporated (Choi et al., 2006) to the mutant *P. aeruginosa* PAO1 strain encoding *qst*. Cells were grown overnight at 37°C on LB agar supplemented with gentamicin (30 μg/mL), carbenicillin (200 μg/mL), 1 mM isopropyl-β-D-1-thiogalactopyranoside (IPTG) and 0.2% L-arabinose (L-ara). Ninety-six colonies were selected and checked for false positive hits by repeating the growth step on selective media. The plasmids of the positive hits were isolated using the GeneJET Plasmid Miniprep Kit (Thermo Scientific) and transformed afresh to the *P. aeruginosa qst* strain to verify if the phenotype is indeed due to the presence of the fragment. After confirmation, a single colony was picked to perform a spot test. From each overnight culture, a hundredfold dilution series was spotted in triplicate on LB agar with or without IPTG/L-ara and overnight incubated at 37°C. To determine the location of the fragments in the *P. aeruginosa* genome, the sequencing results were analysed with Basic Local Alignment Search Tool (BLAST; NCBI (Altschul et al., 1990)) and the *Pseudomonas* Genome Database (Winsor et al., 2016). Individual genes, which were located in the maximal overlap region of the identified fragments, were cloned in the pME6032 vector (Heeb et al., 2002) for electroporation to the *P. aeruginosa qst* strain. Again, a dilution series was spotted on LB with and without 1 mM IPTG and incubated overnight at 37°C. As a negative control, the empty pME6032 vector was used.

Time-lapse microscopy

Microscopic analysis was performed according to a previously described procedure (Wagemans et al., 2014). Briefly, an overnight culture of *P. aeruginosa* cells, containing a single-copy *qst* expression construct and the multicopy expression vector pME6032 with or without bacterial gene, was diluted thousand times and spotted on LB agar supplemented with gentamicin (30 μg/mL), tetracycline (60 μg/mL) and 1 mM IPTG. Time-lapse microscopy was performed for 5 h at 37°C with a temperature controlled Nikon Eclipse Ti time-lapse microscope using the NIS-Elements AR 3.2 software (Cenens et al., 2013).

Protein expression and purification

Qst was fused to a His-tag using the pEXP5-CT/TOPO vector (Thermo Fisher Scientifi c) following the TA-cloning protocol provided by the manufacturer. The bacterial protein PA1217 was fused to a GST-tag by cloning it into a pGEX-6P-1 vector (Cytiva, Marlborough, MA) using the BamHI and EcoRI restriction sites (Thermo Scientific). Recombinant expression of both proteins was performed in exponentially growing *E. coli* BL21(DE3) cells after induction with 1 mM IPTG at 30°C overnight. The proteins were purified using a 1 mL HisTrap HP column (Cytiva) or 5 mL GSTrap HP column (Cytiva), depending on the fused tag, on an Äkta Fast Protein Liquid Chromatography (FPLC, Cytiva) system, followed by dialysis to storage buffer (50 mM Tris-HCl, pH 7.4, 150 mM NaCl) supplemented with 5% (PA1217) or 15% (Qst) glycerol and stored at −20°C.

In vitro pull-down

A total of 250 ng of Qst was incubated with 1 mL Ni-NTA Superflow beads (Qiagen, Hilden, DE) in an end-over-end shaker for 1 h at 4°C. The supernatant was removed by centrifugation at 300 *g* for 5 min and the mixture was suspended in 10 mL pull-down buffer (20 mM Tris pH 7.5, 200 mM NaCl, 20 mM imidazole). The Ni-NTA matrix was loaded on a prepared 1 mL Polypropylene column (Qiagen) and a filtered *P. aeruginosa* cell lysate was added. For the bacterial lysate, cells were grown in 1 L LB until an OD_{600nm}

of 0.6, pelleted and resuspended in 40 mL protein A buffer (10 mM Tris pH 8.0, 150 mM NaCl, 0.1% (v/v) NP-40) supplemented with 40 mg HEWL and 24 mg Pefabloc®SC. Cell lysis was done by three freeze-thaw cycles and sonication (40% amplitude, 8 times 30 sec with 30 sec in between). The column was washed three times with pull-down buffer, after which 500 μL pull-down buffer supplemented with 500 mM imidazole was added. After briefly vortexing the column and 5 min incubation at room temperature, the proteins were eluted by centrifugation at 1,000 *g* for 5 min and visualized using SDS-PAGE. The protein bands that were present in the pull-down sample but absent in the control sample (without loaded Qst) were analyzed using mass spectrometry analysis as described previously (Van den Bossche et al., 2016).

Native mobility shift assay

Interaction between the phage and bacterial protein was evaluated *in vitro* using a native mobility shift assay (Van den Bossche et al., 2014). Mixtures of 200 μM *P. aeruginosa* PA1217 and an increasing amount of Qst were incubated in reaction buffer (20 mM Tris, pH 8) for 10 min at room temperature (T_R). After the addition of loading dye (0.2% (w/v) bromophenol blue, 300 mM DTT and 50% (v/v) glycerol), the samples were loaded on a 10% polyacrylamide native gel (10% (v/v) 37.5:1 acrylamide/bisacrylamide, 10% (v/v) glycerol, 200 mM Tris, pH 8, 0.01% (v/v) APS, 0.001% (v/v) TEMED) and run in running buffer (25 mM Tris, 250 mM glycine) for 80 min at 150 V. The gel was Coomassie-stained, the shifted bands were excised from the gel and the gel pieces were loaded on a 12% SDS-PAGE gel to confirm the presence of both proteins. Furthermore, the proteins were identified using mass spectrometry analysis as described previously.

Enzyme-linked immunosorbent assay (ELISA)

ELISA was performed using anti-GST coated strips (Pierce™ Anti-GST Coated Clear Strip Plates, Thermo Fisher Scientific). A fixed amount of 10 pmol GST-tagged PA1217 was diluted in 200 μL PBS (137 mM NaCl, 2.7 mM KCl, 8.2 mM Na_2HPO_4, 1.8 mM KH_2PO_4, pH 7.5) supplemented with 2% (w/v) Bovine serum albumin (BSA), added to the wells and incubated for 1 h at room temperature while gently shaking. After washing the wells three times with PBS-Tween 0.1% followed by three times PBS, increasing amounts of His-tagged Qst were diluted in 200 μL PBS +2% BSA, added to the wells and incubated for 1 h at room temperature. The washing step was repeated and 200 μL of a 1:5,000 dilution of the monoclonal Anti-His antibody (Sigma-Aldrich, St. Louis, MO) in PBS +2% BSA was added to each well. After incubating 1 h at T_R, the wells were washed and 200 μL of a 1:5,000 dilution of secondary Anti-Mouse IgG antibody conjugated to HRP (Promega Corporation, Madison, WI) in PBS +2% BSA was added to each well. A final washing step after 1 h incubation at T_R was followed by addition of 100 μL 1-Step Slow TMB-ELISA substrate (Thermo Scientific) to each well and absorbance was measured after 10 min incubation at room temperature using the Bio-Rad Model 680 Microplate Reader (655 nm; Bio-Rad, Hercules, CA). As negative controls, wells without bait protein (GST-tagged PA1217) and pure GST tag were used. Three replicates of each combination were tested.

Bacterial two-hybrid

Bacterial two-hybrid assays were conducted using the BACTH System kit (bacterial adenylate cyclase two-hybrid system kit, Euromedex). The *P. aeruginosa* genes *PA1217, pqsD* and *thiD* were cloned into four vectors (pUT18, pUT18C, pKT25 and pN25), while the fragments of the former (sequences encoding amino acid 1–259, 1–342, 97–317, 156–342 and 260–455) were only cloned into pKT25. The *P. aeruginosa* genes *coaC, pqsB* and *pqsC* were cloned into vectors pKT25 and pN25, and the phage gene *qst* was cloned into the vectors pUT18, pUT18C and pN25. Each combination of phage and bacterial gene/fragment was co-transformed to *E. coli* BTH101 and dilutions of overnight cultures were spotted on synthetic minimal M63 medium (15 mM $(NH_4)_2SO_4$, 100 mM KH_2PO_4, 1.7 μM $FeSO_4$, 1 mM $MgSO_4$, 0.05% (w/v) vitamin B1, 20% (w/v) maltose) supplemented with 0.5 mM IPTG and 40 μg/mL 5-bromo-4-chloro-3-indolyl-β-D-galactopyranoside (X-gal). To quantify the β-galactosidase activity, Miller assays were performed (Zhang and Bremer, 1995). As negative controls, the constructs were co-transformed with their empty counterparts. Each combination was tested in triplicate.

CoA acetyltransferase activity assay

To measure acetyl-CoA dependent acetyltransferase activity of the bacterial and phage protein, an endpoint assay was performed as previously described (Roucourt et al., 2009). Briefly, the formation of CoA was determined using 5,5′-dithiobis-(2-nitrobenzoic acid) (DTNB), which reacts with free thiol groups of CoA. Mixtures of 1 μg PA1217 and/or 5 μg Qst, 2 mM 3-methyl-2-oxobutanoic acid (Fisher Scientific, Hampton, NH) and 1 mM acetyl-CoA (Sigma-Aldrich) were incubated in a reaction buffer (70 mM Tris, pH7.5, 3.5 mM $MgCl_2$, 3.5 mM KCl) for 30 min at 37°C. After the addition of 2 mM DTNB (Sigma-Aldrich) to each sample, the absorption was measured at 415 nm in a microplate reader (Microplate reader model 680, Bio-Rad). As a positive and negative control, samples with LeuA and without protein and pure GST tag were tested, respectively. The experiment was performed in triplicate.

^{1}H-NMR analysis

The predicted α-isopropylmalate synthase activity of PA1217 was studied using ^{1}*H-NMR* (de Carvalho and Blanchard, 2006). Mixtures of 100 μg PA1217, 12 mM $MgCl_2$, 1.1 mM 3-methyl-2-oxobutanoic acid and 1 mM acetyl-CoA were incubated in 50 mM potassium phosphate buffer (pH 7.5) for 2 h at 37°C. The proteins were removed using Amicon Ultra 3K 0.5 mL centrifugal filters (Millipore, Burlington, MA) according to the manufacturer's protocol. Lastly, 300 μL of D_2O was added to 300 μL of the prepared mixture. ^{1}*H-NMR* spectra were recorded on a Bruker Ascend 600 MHz and 400 MHz spectrometer equipped with a BBO 5 mm atma probe

and a sample case. To suppress the broad signal of water, an adapted zgpr pulse program (p1 9.75 μs; plw1 15W; plw9 5.7–05W; o1P) was applied on the resonance signal of water, which was determined and selected automatically. The experiment was repeated with mixtures containing Qst, a combination of Qst and PA1217, and the positive control LeuA.

Metabolomics using FIA-qTOF-MS

Metabolites were extracted from *P. aeruginosa* cells and analyzed following the procedure described previously (De Smet et al., 2016). Cells were grown until an OD_{600nm} of 0.1, 1 mM IPTG was added to each culture and sampling was done every 15 min. Four strains were tested: PAO1 wild type, PAO1 encoding *qst*, PAO1 containing the multicopy expression vector pME6032 with PA1217 gene, and PAO1 combining the previous two strains. The samples were analysed using negative mode flow injection-time-of-flight mass spectrometry (FIA-qTOF). Ions were annotated with KEGG *P. aeruginosa* metabolite lists (Kanehisa and Goto, 2000), allowing a mass tolerance of 1 mDa and an intensity cutoff of 5,000 counts. Raw intensities were quantile normalized (each measurement is an average of two technical replicates) and fold changes were calculated for each time point between each condition and control for means of three biological replicates and reported in log2. p values were calculated with unpaired t test and corrected for multiple hypothesis testing with Benjamini-Hochberg procedure. Page's trend test p values were calculated using the Matlab Page package: http://www.mathworks.com/matlabcentral/fileexchange/14419-perform-page-test?focused=6141676&tab=function.

Bioassay

The effect of the phage and bacterial protein on the production pattern of PQS autoinducer by *P. aeruginosa* was tested using the *P. aeruginosa* PAO1-R1 (pTS400) reporter strain (Van Houdt et al., 2004). First, cell-free culture supernatants from tested *P. aeruginosa* strains were prepared as described by Van Houdt et al. (2004) with some modifications. Briefly, overnight cultures of *P. aeruginosa* cells (over)expressing the *qst* and/or the PA1217 gene were diluted (1:100) in fresh LB medium and grown for 21 h at 37°C. The cells were then removed by centrifugation (24,000 *g*) for 10 min and cleared supernatants was filtered using 0.22 μm Millex filter units (Millipore). Next, 2 mL of the cell-free culture supernatant was mixed with 2 mL of freshly diluted (1:100) *P. aeruginosa* PAO1-R1 (pTS400) culture in PTSB medium (5% (w/v) peptone, 0.25% (w/v) trypticase soy broth), and incubated for 18 h at 37°C. The production of reporter enzyme β-galactosidase was measured using previously mentioned Miller assay (Zhang and Bremer, 1995). The experiment was performed in triplicate.

Thin-layer chromatography

The alkyl quinolones PQS and HHQ were extracted from *P. aeruginosa* cells and analyzed by thin-layer chromatography (TLC) following the procedure described by Fletcher et al. (2007) with modifications. First, overnight cultures of *P. aeruginosa* cells containing the *qst* gene or an empty construct were diluted (1:100) in fresh PTSB medium. The 4-mL cultures were induced with different IPTG concentrations (0 μM, 5 μM, 10 μM, 50 μM, 1 mM IPTG) and incubated for 24 h at 37°C. The alkyl quinolones were subsequently extracted from 500 μL supernatants by adding equal volumes of acidified (0.015% (v/v) glacial acetic acid) ethyl acetate twice (double extraction). The organic phase was dried in a vacuum centrifuge and the solute was dissolved in 20 μL methanol. For each condition, 2 μL sample was spotted on silica 60 F254 TLC plate (Merck), pre-treated by soaking in 5% K_2HPO_4 for 30 min and activated at 100°C for 1 h. As controls, 2 μL of 10 mM synthetic PQS and HHQ (Sigma-Aldrich) were spotted. The plate was placed in a 95:5 dichloromethane:methanol solvent for 10 min to separate the extracts, and the alkyl quinolones were visualized under UV light.

Phage infection assays

After determining the phage titer using the standard soft agar overlay method and counting the number of plaque forming units (pfu) per ml, a spot test on *P. aeruginosa* PAO1 strain and derived deletion mutants was performed. For this, 200 μL bacterial overnight culture was mixed with 4 mL soft agar and poured over solid LB to create a bacterial lawn. A phage dilution containing approximately 10 pfu (1 μL) was spotted on the top of this double agar, followed by overnight incubation at 37°C. Infection curves were determined by measuring the OD_{600nm} every 10 min during 100 min using the Novaspec®II spectrophotometer (Pharmacia, Freiburg, DE) after infecting the *P. aeruginosa* cells at OD_{600nm} of 0.3 with 10 times excess of phages compared to bacterial cells.

QUANTIFICATION AND STATISTICAL ANALYSIS

All information regarding the statistical analysis including number of repeats (n), standard deviations and p values, as well as the types of statistical test used can be found in the figure legends and/or method details. More specifically, the Student's t-test was used for analyzing significant differences between the Enzyme-linked immunosorbent assay results (Figure 2B), the Miller Assay results of the Bacterial two-hybrid analyses (Figures 2C, 5, and S2), and the CoA acetyltransferase activity assay results (Figure 3). Standard deviations were also calculated for these results, as well as for the Miller Assay results of the bioassay (Figure S4B) and for the phage infections results (Figure 6). The standard deviations are represented with error bars in the respective figures. All the above-mentioned calculations were performed in MS Excel. For the metabolomics, four biological replicates were sampled and two technical repeats were made of each sample. For each ion, the metabolite with the highest annotation score was used, and for each annotated metabolite, only the annotation of the best score was kept. The statistical analysis was performed using Matlab R2013b, as described in Table S1 and the method details (Figures 4 and S4A, Table S1).